9 First Principles Theory of Mantle and Core Phases

Lars Stixrude

Department of Geological Sciences
425 E. University Avenue
University of Michigan
Ann Arbor, Michigan, 48109-1063, U.S.A.

INTRODUCTION

The Earth's interior is an extreme environment where the pressure and temperature (up to 3.6 Mbar or 360 GPa, and approximately 6000 K, respectively at Earth's center) are sufficiently high to affect the structure, physics, and chemistry of minerals in often surprising ways that may confound our intuition based on studies at near-ambient conditions. Though the Earth's interior deeper than 12 km has not been subject to *in situ* observation, observational evidence from seismology, combined with experimental and theoretical studies of Earth materials under extreme conditions, has allowed us to construct a picture of this remote region of the planet (Fig. 1). Although the mineralogy of the uppermost mantle is familiar from studies of xenoliths, the deepest portion of the silicate mantle (2890 km depth, or 136 GPa) is more than twice as dense as average continental crust (Dziewonski and Anderson 1981), and is thought to be composed primarily of a phase not yet seen at the Earth's surface: an Mg-rich meta-silicate with the perovskite structure. The Earth's core is thought to be composed primarily of iron and is subdivided into a liquid outer part and a solid inner part. The inner core is 65% denser than iron at ambient conditions, partly due to the effects of compression, and partly to the stabilization, at high pressure, of a close-packed, paramagnetic phase of iron.

Over the regime of the Earth's interior, pressure has a larger effect than temperature on the density and many other physical properties. It is in part for this reason that most high pressure studies of minerals have been performed at ambient or zero temperature. One can show on general grounds that the pressure in the Earth is sufficiently large that one must expect substantial changes in the electronic structure of minerals within the Earth's interior. In addition to structural solid-solid phase transformations, one expects changes in the nature and character of bonding, from ionic, towards increasing covalency, or from insulating to metallic behavior. The richness of the microscopic physics of the deep interior places tremendous demands on theoretical methods. First principles methods, and in particular density functional theory, the focus of this review, are uniquely suited to the study of minerals at extreme conditions because they are equally applicable to all types of structures and bonding, and to all elements in the periodic table. A review of first principles methods as they have been applied in the context of high pressure mineral physics and geophysics is given in Stixrude et al. (1998).

Although the influence of temperature is secondary to that of pressure, it is central to our understanding of geodynamics. In the broadest terms, the thermal evolution of the Earth is manifested in the dynamic processes of plate tectonics, volcanism, and others, through the influence of temperature on the physical and chemical properties of minerals. A fundamental concern is an understanding of how temperature affects thermodynamic properties and phase equilibria, including solid-solid phase transitions, melting, and devolatilization. In the lithosphere, where the geothermal gradient is large and highly variable, temperature has a strong influence on physical properties, and through igneous processes, is ultimately responsible for the presence of the crust. Below the lithosphere,

1529-6466/00/0042-0009$05.00

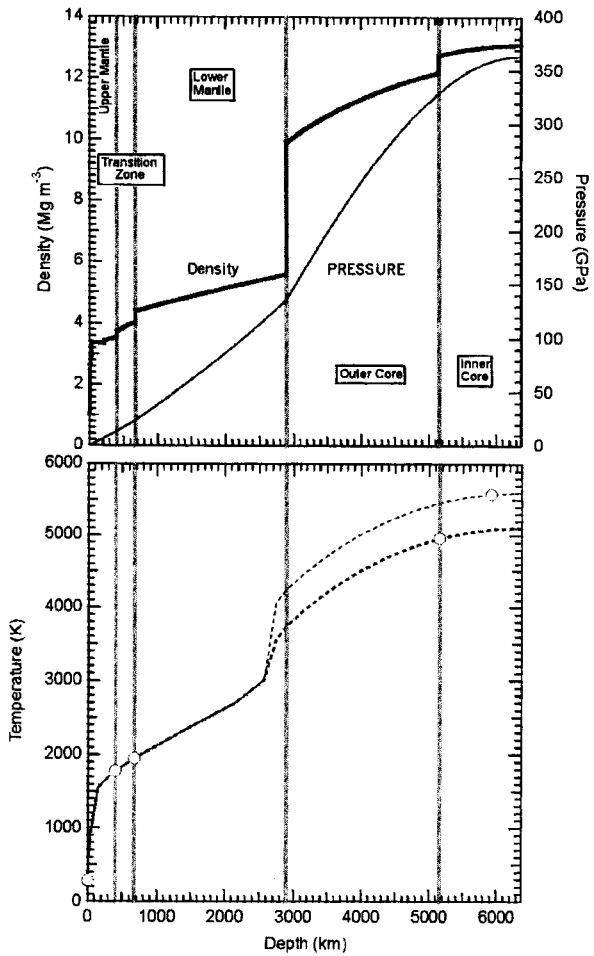

Figure 1. Properties of the Earth's interior: the density (bold line) as determined seismologically and the pressure (light line) calculated from the density distribution (Dziewonski and Anderson 1981). The density profile reflects the divisions of the Earth's interior into mantle and core and the further subdivision into upper mantle, transition zone, and lower mantle, liquid outer core, and solid inner core. The temperature distribution cannot be directly observed below the uppermost crust and must be inferred. The bold dashed line is due to Stacey (1992). Fixed points along the geotherm (symbols) are depths at which the average temperature may be estimated by comparing seismological observations with experimental or theoretical determinations of the properties of Earth materials. For example, the two points within the mantle derive from determinations of the Clapeyron slope of solid-solid phase transformations that account for the sudden change in seismic properties at the boundaries between upper mantle, transition zone and lower mantle. The point at the inner core boundary is based on experimental determination of the iron melting curve and estimates of the effects of freezing point depression due to light alloying constituents in the core. The point within the inner core is from a new constraint on deep Earth temperatures discussed in this review (Steinle-Neumann et al. 2000). The discrepancy between this determination of inner core temperatures and that based on the iron melting curve is illustrative of the uncertainties that likely remain in our knowledge of the geotherm. In some parts of the earth, temperature may also vary laterally (not shown). In the mantle, lateral temperature variations drive mantle convection and may exceed 1000 K; see e.g., Davies (1999) for an introduction to mantle dynamics. In the outer core, temperature varies little laterally (Stevenson 1987), and the inner core is probably isothermal to within a few hundred degrees (Stixrude et al. 1997).

the geothermal gradient is greatly reduced, approximating an adiabat, and lateral variations in temperature are smaller. Although the resultant lateral variations in physical properties are comparatively subtle, they are directly responsible for the largest scale dynamic processes in the planet; lateral density variations (buoyancy) being the driving force for mantle convection. In the Earth's core, isolated from the Earth's surface and from direct observation, an understanding of the effects of pressure and temperature on the properties of materials is an essential component of our knowledge of the composition of this region.

The theoretical treatment of the behavior of materials in the Earth's interior requires two major ingredients. First is the calculation of the total energy of a fixed arrangement of nuclei and their complementary electrons. This calculation requires powerful quantum mechanical methods because the range of elements, structures, and bonding environments encountered within the Earth is large. Second is the sampling of configuration space; that is the efficient enumeration of energetically important states of the crystal as its constituent atoms undergo thermal vibration or other types of motion (e.g., diffusion). The most commonly used approach is molecular dynamics, which makes use of additional physical quantities such as the force acting on the atoms. While first principles methods for computing the total energy and molecular dynamics have both been in use for decades, their combination is quite recent, dating from the work of Car and Parrinello (1985).

We begin with an outline of the nature of the problem, emphasizing the unique aspects of temperature and its physical effects from a theoretical point of view. A brief overview of some essential aspects of statistical mechanics follows which serves as a foundation from which all practical methods follow. This overview will emphasize the total energy as a fundamental concept and object of calculation and the efficient sampling of configuration space as a primary concern. First principles methods for computing the total energy, as well as forces and stresses are described. Methods for sampling configuration space are compared, including Monte Carlo, molecular dynamics, and the cell model, a simplified physical model that serves to illuminate the physics. Some applications follow, to the major materials of the Earth's mantle and core, and some future prospects are discussed.

THEORY

Overview

The nature of the problem. Consider a monatomic one-dimensional crystal (Fig. 2). Imagine the state of the crystal under static conditions, in which the temperature is zero and zero-point motion is absent. Note that this state is inaccessible in the laboratory; whereas temperatures close to absolute zero may be achieved, zero-point motion cannot be eliminated. In this idealized situation, the atoms are stationary and occupy ideal crystallographic sites. The resulting structure possesses high symmetry and a small unit cell. From a theoretical point of view, these are desirable properties. We are able to apply periodic boundary conditions, and the period is small. These properties are unique to the static crystal and account for the importance of this idealization in theoretical studies.

Now consider the same crystal at finite temperature. Recall that the temperature is defined as the average kinetic energy of the atoms. Temperature therefore implies motion: at any instant, it will be highly unlikely to find any atom occupying an ideal crystallographic site. Consider a snapshot of our crystal in which a single atom is displaced. Because the ideal crystallographic site is defined as a state of lowest energy, the potential energy in the displaced position must be greater. This energy of

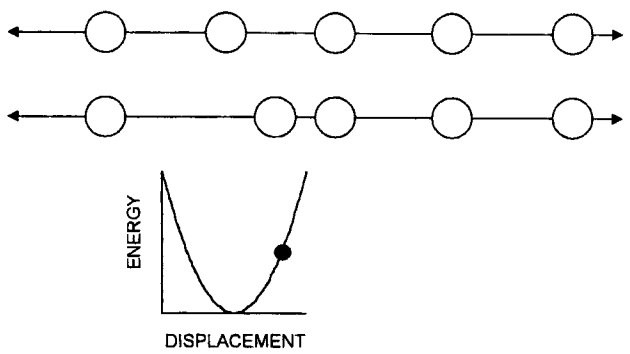

Figure 2. The nature of the statistical mechanical problem in the case of a crystalline solid. Uppermost is a representation of a perfect one-dimensional monatomic lattice as would exist under static conditions. Immediately beneath is an illustration of the effect of temperature; atoms no longer occupy their ideal lattice sites and the symmetry of the structure at any instant is completely broken. The lowermost graph shows how the energy of the structure depends on the displacement of an atom; the dependence is quadratic to first order, but higher order (anharmonic) terms may be important at conditions typical of the Earth's interior.

displacement leads to thermodynamic properties including, for example, thermal expansivity and heat capacity. The dependence of the energy on the magnitude of the displacement gives rise to a force acting on the atom, in this case a restoring force that tends to return the atom to its ideal site. At high temperature, we have a formidable theoretical problem. The symmetry of any snapshot of the structure is completely broken and the unit cell is infinitely large.

Statistical mechanics. Statistical mechanics provides the tools required to deal with the physics of materials at high temperature. There are many excellent introductory texts for the interested reader (Hill 1956; Landau and Lifshitz 1980; McQuarrie 1976; Reif 1965). We focus on equilibrium thermodynamic properties because these play such an important role in our understanding of the Earth's interior. For the purposes of this discussion, we require a single result of statistical mechanics: the partition function of a system of N atoms

$$Q = \frac{1}{N!\Lambda^{3N}} \int \exp\left[-E(\mathbf{R}_1, \mathbf{R}_2, ..., \mathbf{R}_N)/kT\right] d\mathbf{R}_1 d\mathbf{R}_2 ... d\mathbf{R}_N \quad (1)$$

is a $3N$-dimensional integral over the coordinates of the atomic nuclei, located at $\mathbf{R}_i$. The thermal de Broglie wavelength $\Lambda = h/\sqrt{(2\pi mkT)}$ where h is the Planck constant, k the Boltzmann constant, and m the nuclear mass. The integrand depends on the total energy E and the temperature T. The total energy is a unique function of the coordinates of the atomic nuclei. This formulation of the problem is exact at temperatures sufficiently high that classical statistics are applicable to the atomic motions. A criterion for the applicability of our classical treatment is the value of Λ, which can be thought of roughly as the spatial extent of the wavefunction of the atomic nucleus. Classical statistics are applicable as long as Λ is much less than the average interatomic spacing. Another test of classical behavior is that the temperature must exceed the Debye temperature, a measure of the typical vibrational frequency of a material (Dove 1993; Kieffer 1979). This condition is met throughout most of the Earth's interior where typical temperatures in the mantle and core (~3000 K and ~6000 K respectively) are substantially greater than the

Debye temperatures of their most abundant constituents (~1000 K and ~300 K, respectively).

Once we have evaluated the partition function, all thermodynamic properties follow. The Helmholtz free energy for example is

$$F = -kT \ln Q \quad (2)$$

Other thermodynamic properties are simply related to volume and temperature derivatives of F (Callen 1960). For example, the pressure (negative of the volume derivative) can be calculated by computing the Helmholtz free energy at two different values of the volume.

In order to explore material properties at lower temperatures, first order quantum corrections may be computed. Lattice dynamics is a complementary approach, valid in the limit of low temperature (see Parker et al., this volume). The periodicity of the lattice is used to elegant advantage, leading to the concept of phonon dispersion. In this method, the total energy is expanded to second order in the atomic displacements, and the energetics of vibrational excitation are explored with the proper quantum statistics. The critical limitation of the lattice dynamics method is the quasiharmonic approximation; higher order terms in the expansion of the total energy are neglected. The method may fail at high temperatures where atomic displacements can be large and anharmonic contributions to thermodynamic properties correspondingly important.

In metals and semi-conductors, the thermal excitation of electrons must also be considered. We may write the Helmholtz free energy

$$F = E(V,T) - TS_{el}(V,T) + F_{vib}(V,T) \quad (3)$$

where the total energy, E, is now a function of temperature, S_{el} is the entropy arising from the thermal excitation of electrons and F_{vib} is the vibrational portion of the free energy. In the special case of an insulator, S_{el}=0 and F_{vib}=F-$E(V,0)$. The total energy at finite temperature must be determined self-consistently with the charge density. This is because the thermal excitation of electrons alters the charge density, and in turn the potential to which the electronic states respond. The thermal excitation of electrons must be treated with the proper quantum statistics since the relevant energy scale, the Fermi temperature (130,000 K in the case of iron) is much higher than the Debye temperature. The Fermi temperature is the energy of the highest energy electronic state divided by k (Kittel 1996). The partition function of a metal or semi-conductor is computed using Equation (1), but with the total energy replaced by the electronic free energy

$$Q = \frac{1}{\Lambda^{3N} N!} \int \exp\left[-F_{el}(\mathbf{R}_1, \mathbf{R}_2, ...\mathbf{R}_N; T)/kT\right] d\mathbf{R}_1 d\mathbf{R}_2 ... d\mathbf{R}_N \quad (4)$$

$$F_{el}(\mathbf{R}_1, \mathbf{R}_2, ..., \mathbf{R}_N; T) = E(\mathbf{R}_1, \mathbf{R}_2, ..., \mathbf{R}_N; T) - TS_{el}(\mathbf{R}_1, \mathbf{R}_2, ..., \mathbf{R}_N; T) \quad (5)$$

where the dependence of the electronic free energy on temperature is made explicit. This expression reduces to (Eqn. 1) in the limit of large band gaps. In the analysis that follows, we will assume that we are dealing with insulators and that the special case (Eqn. 1) applies, while recognizing that the generalization to metals is straightforward.

For the statistical mechanical problem to be well posed, a choice of ensemble is essential. To this point, we have assumed the canonical or NVT ensemble, that is one in which the number of particles, N, the volume, V, and the temperature T are held constant, while the conjugate variables: chemical potential, pressure, and energy are allowed to fluctuate. The magnitude of these fluctuations can be related to thermodynamic

properties. For example, energy fluctuations are related to the heat capacity (McQuarrie 1976). Other ensembles are also possible. As we will see, the *NVE* or micro-canonical is the natural ensemble of molecular dynamics. The *NPT* ensemble, where *P* is the pressure, is perhaps the most convenient for comparison with experiment because these are the variables that are generally controlled in the laboratory. In this ensemble, the volume, or more generally, the cell-shape fluctuates. The development of variable cell-shape methods in statistical mechanics has been a major advance in the study of the large number of Earth materials that have less than cubic symmetry (Wentzcovitch 1991; Wentzcovitch et al. 1993). In this ensemble, the partition function differs from (Eqn. 1) in that an integral over all possible volumes is also included.

Regardless of the ensemble chosen, we are faced with evaluating the integral of Equation (1) or one of similar dimensionality. We must generate, in principle, all possible atomic arrangements (snapshots) of the system and evaluate the total energy (or electronic free energy in the case of metals) for each. Because the integral contains so many dimensions, $O(10^{23})$, this brute force approach is impossible. More efficient methods for solving the statistical mechanical problem, including the particle in a cell method, the Monte Carlo method, and the molecular dynamics method are discussed below. First we focus on the computation of the total energy for a given arrangement of nuclei, which is essential for all these methods, and the computation of forces and stresses, which is the basis of molecular dynamics.

Total energy, forces, and stresses

A wide range of theoretical methods for computing the total energy have appeared in the Earth sciences literature, and many have been applied to understanding the behavior of deep Earth materials. These methods differ greatly in the level of physics included and as a result in the quality and security of their predictions. First principles methods lie at one extreme of the theoretical spectrum and are distinguished by containing i) the smallest possible number of approximations and ii) no free parameters. Because they are most closely tied to the fundamental physics, first principles methods have the greatest predictive power. This is particularly important in the study of the earth's deep interior where conditions of pressure and temperature exceed those that can be routinely reproduced in the laboratory. Two classes of first principles methods have been important in the study of deep earth materials. The Hartree-Fock method is discussed elsewhere in this volume. Our focus will be on density functional theory which has the advantage of being equally applicable to all elements of the periodic table and to all types of bonding. Other theoretical methods, which are computationally more efficient, but whose predictive power is less than first principles methods, exist. The term *ab initio* is applied to those methods that, while parameter free and independent of experiment, construct an approximate model of some aspect of the relevant physics. An example is the electron gas method of Gordon and Kim (1972) and its successors, in which the charge density is modeled by overlapping spherically symmetric atomic or ionic charge densities. Semi-empirical methods rely on experimental measurement for the values of free parameters. One example is the Born-Mayer rigid ion model (see Born and Huang 1954 for an extended discussion), in which the potential energy is represented as a sum of pair-wise inter-atomic interactions. See Stixrude et al. (1998) for a more complete comparison of first principles with other methods.

From the point of view of any first principles theory, solids are composed of nuclei and electrons; atoms and ions are constructs that play no primary role. This departure from our usual way of thinking about minerals is essential and has the following important consequences. We may expect our theory to be equally applicable to the entire range of conditions encountered in planets, the entire range of bonding environments

entailed by this enormous range of pressures and temperatures, and to all elements of the periodic table. Because there are no free parameters, first principles calculations have no input from experiment and are therefore ideally complementary to the laboratory effort.

Density functional theory is a powerful and in principle exact method of solving the quantum mechanical problem that has revolutionized the theoretical study of condensed matter (Hohenberg and Kohn 1964; Kohn and Sham 1965), see Jones and Gunnarsson (1989) for a review. The essence is the proof that the ground state properties of a material are a unique functional of the charge density $\rho(\mathbf{r})$. This is important theoretically because the charge density, a scalar function of position, is a much simpler object than the total many-body wavefunction of the system. The total energy

$$E[\rho(\mathbf{r})] = T[\rho(\mathbf{r})] + \frac{1}{2}\sum_{i,j}\frac{Z_i Z_j}{|\mathbf{R}_j - \mathbf{R}_i|} + \sum_i \int \frac{Z_i \rho(\mathbf{r})}{|\mathbf{R}_i - \mathbf{r}|} d\mathbf{r} + \int \frac{\rho(\mathbf{r})\rho(\mathbf{r}')}{|\mathbf{r}' - \mathbf{r}|} d\mathbf{r} d\mathbf{r}' + E_{xc}[\rho(\mathbf{r})] \quad (6)$$

The first term T is the kinetic energy of a system of non-interacting electrons with the same charge density as the interacting system. The next three terms are the electrostatic (Coulomb) energy of interaction: i) among the nuclei; with charge Z_i and location $\mathbf{R}_i$, ii) between nuclei and electrons and iii) among the electrons, the so-called Hartree term. The last term E_{xc} is the exchange-correlation energy which accounts for physics not included in the Hartree contribution, including the tendency of electrons to avoid each other because of their like charges and the Pauli exclusion principle. The power of density functional theory is that it allows one to calculate, in principle, the exact charge density and many-body total energy from a set of single-particle equations: the so-called Kohn-Sham equations

$$\left\{-\nabla^2 + V_{KS}\left[\rho(r)\right]\right\}\psi_i = \varepsilon_i \psi_i \quad (7)$$

where ψ_i is the wave function of a single electronic state, ε_i the corresponding eigenvalue and V_{KS} is the effective potential that includes Coulomb terms and an exchange-correlation contribution, V_{xc}. Because the potential is itself a functional of the charge density, the equations must be solved self-consistently, usually by iteration.

The Kohn-Sham equations are exact. They cannot be solved exactly however, because we do not yet know the exact, universal form of the exchange-correlation functional. Fortunately, simple approximations have been very successful. The Local Density Approximation (LDA) is based on the precisely known case of the uniform electron gas. The LDA takes into account nonuniformity of the charge density in real materials to lowest order by setting V_{xc} at every point in the crystal to that of the uniform electron gas with a density equal to the local charge density (Lundqvist and March 1987). The LDA has been shown to yield excellent agreement with experiment for a wide variety of materials and properties, but also shows some important flaws; for example, it fails to predict the correct ground state of iron. The shortcomings of the LDA may be due to its local character, that is, its inability to distinguish between electrons of different angular momenta or energy. Generalized gradient approximations (GGA) partially remedy this by including a dependence on local charge density gradients in addition to the density itself (Perdew et al. 1996).

In addition to the essential approximation to the exchange-correlation functional, some first principles calculations make additional assumptions that are asymptotically

valid. These include the frozen core approximation, and the pseudopotential approximation. There are a number of excellent reviews of the pseudopotential concept and its applications (Cohen and Heine 1970; Heine 1970; Pickett 1989). The physical motivation for the frozen core approximation is the observation that only the valence electrons participate in bonding and in the response of the crystal to most perturbations of interest. We then need solve only for the valence electrons in Equation (7), often a considerable computational advantage. The pseudopotential approximation goes one step further by replacing the nucleus and the frozen core electrons with a simpler object, the pseudopotential, that has the same scattering properties. The advantages of the pseudopotential method are 1) spatial variations in the pseudopotential are much less rapid than the bare Coulomb potential of the nucleus and 2) one need solve only for the (pseudo-) wavefunctions of the valence electrons which show much less rapid spatial variation than the core electrons, or the valence electrons in the core region. This means that in the solution of the Kohn-Sham equations, potential and charge density can be represented by a particularly simple, complete and orthogonal set of basis functions (plane-waves) of manageable size. The construction of the pseudopotential is non-unique. Care must be taken to demonstrate the transferability of the pseudopotentials generated by a particular method and to compare with all electron calculations where these are available. When these conditions are met, the error due to the pseudopotential is generally small (few percent in volume for Earth materials) (Stixrude et al. 1998).

First principles methods yield the total energy, the charge density, and the quasi-particle eigenvalue spectrum (band structure) for a given (static) arrangement of nuclei. The total energy is not only an important ingredient in our central problem (Eqn. 1), but is also a quantity of interest in itself. By examining changes in the total energy with respect to perturbations of the crystal structure, we make contact with experimental measurements. For example, the change in the total energy with respect to volume yields the equation of state. Calculations of the total energy in strained configurations can be used to determine the elastic constants. These properties are of course for the static lattice, which is not observable experimentally. However, it is a useful idealization for comparison with laboratory measurements at ambient conditions where thermal effects are small for many materials and properties.

In addition to the total energy, it is possible directly to calculate first derivatives of the total energy using the Hellman-Feynmann theorem (Feynman 1939; Hellman 1937). The application of this theorem allows one to determine the forces acting on the nuclei and the stresses acting on the lattice (Nielsen and Martin 1985). This is important for several reasons. The most important in the context of high temperature behavior is that knowledge of the forces and stresses allow us to perform first principles molecular dynamics, a powerful way of solving the statistical mechanical problem. Molecular dynamics is discussed in more detail below. See Payne et al. (1992) for a review of the application of density functional theory to molecular dynamics.

Statistical mechanics

Any of the methods described in the previous section permit the evaluation of the energy that appears in our central problem (Eqn. 1). Recognizing that a naïve attempt to evaluate the partition function directly will fail, we must develop methods that sample configuration space efficiently. An important observation is that of all possible configurations of the nuclei ($\mathbf{R}_1$, $\mathbf{R}_2$, ..., $\mathbf{R}_N$), only a small fraction will contribute significantly to the integral. For any condensed phase, the vast majority of configurations will consist of very high energy states in which pairs of atoms are nearly coincident. Since these states will occur with only vanishingly small probability in nature, our sampling of configuration space must be directed towards the small subset of structures in which

inter-atomic distances are not extremely unfavorable energetically. In the particle-in-a-cell method, a particularly simple and illustrative solution arises from the intentional restriction of our sampling of configuration space to the motion of a single atom. The Monte Carlo method provides an efficient means of sampling configuration space more generally and for the computation of certain thermodynamic quantities. The method of molecular dynamics takes a different approach that allows us to explore not only bulk thermodynamic properties, but also microscopic mechanisms of change.

Particle in a cell method. This method was originally developed as an approximation to the liquid state. However, it was soon realized, in part because the method neglects an explicit treatment of the configurational entropy, that the method was better suited to solids (Cowley et al. 1990; Holt et al. 1970). There are two central approximations. The first recognizes that motion of the atoms in a crystal consists primarily of vibration about ideal crystallographic sites. While diffusion and the formation of defects are important for understanding deformation and transport properties, their contribution to thermodynamic properties is secondary. Space is divided into non-overlapping sub-volumes centered on the nuclei (Wigner-Seitz cells) and the coordinates of each atom restricted to its cell.

The second approximation in the particle in a cell method is that the motion of the atoms are uncorrelated. This is expected to be a good approximation at high temperature where the kinetic energy of vibration is large. If the change in total energy upon moving one atom be independent of the location of the others, then the partition function simplifies tremendously: the $3N$-dimensional integral reduces to the product of N identical 3-dimensional integrals

$$Q = \Lambda^{-3N}\left\{\int_{\Lambda}\exp\left[-\frac{E(\mathbf{R}_1)}{kT}\right]d\mathbf{R}_1\right\}^N \tag{9}$$

where $\mathbf{R}_1$ is the location of the so-called wanderer atom, and Δ is the Wigner-Seitz cell. This type of simplification, an example of the factorization of the partition function, also plays a central role in the analysis of the ideal gas where the particle energies are mutually independent. Note that in the case of our crystal, the factor $N!$ no longer appears because we have assumed that the nuclei can be distinguished by the lattice site about which they vibrate.

The particle in a cell method is a classical mean field approximation in which the wanderer moves in the crystal potential of the otherwise ideal lattice. Because large displacements of the wanderer atom are included in the integral - up to the boundary of the Wigner-Seitz cell, or approximately half the nearest-neighbor distance - the particle in a cell method accounts explicitly for anharmonicity (Fig. 3). The method is very efficient and is much more rapid than Monte Carlo or molecular dynamics. This is a tremendous practical advantage especially when using first principles methods for computing the total energy. The speed of the calculation depends on the number of total energy calculations. These can be reduced considerably, compared with a naïve evaluation of the integral, by using the point symmetry of the wanderer site (Wasserman et al. 1996b).

Practical issues in the implementation of the particle in a cell model include convergence of the total energy of wanderer displacement. There are two distinct convergence issues. One is common to any total energy calculation. The total energy must be converged with respect to the size of the basis set that is used to represent charge density and potential and the number of points in reciprocal space (k-points) at which the Kohn-Sham equations are evaluated (Brillouin zone sampling) (see Stixrude et al. 1998 for an extended discussion). The other convergence issue has to do with the size of the

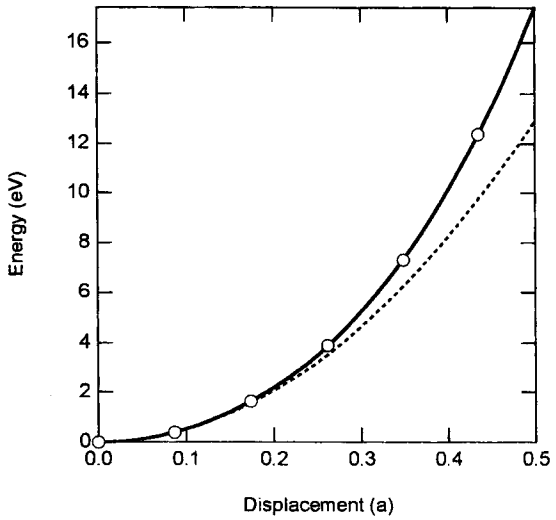

Figure 3. The energy of displacement of one atom in hcp iron at a density of 13 Mg m^{-3} (Steinle-Neumann et al. 2000) (symbols). The atom is displaced along the a-axis directly towards one of the nearest neighbors; magnitude of displacement is measured in units of the *a* lattice parameter. The solid line is a quartic fit. A quadratic fit (dashed line) illustrates the magnitude of anharmonicity.

supercell. Because we retain periodic boundary conditions, we must ensure that the supercell be sufficiently large that the wanderer does not interact with its periodic images. Convergence is demonstrated by computing the change in the total energy for one particular displacement of the wanderer atom as a function of supercell size. Convergence may be achieved for a supercell of ~50 atoms. The two convergence issues are not independent. As the size of the supercell grows, the size of the Brillouin zone shrinks. This means that convergence of the total energy will require evaluation at fewer reciprocal space points (k-points) than would be required of a primitive cell. Indeed, experience shows that calculations with 1-4 k-points are often sufficient even for those cases, such as iron, where hundreds of k-points are required for convergence of the total energy using a primitive unit cell.

As an example of the application of this method, we show results from a study of close-packed iron at high pressure and temperature (Wasserman et al. 1996b) (Fig. 4). The vibrational partition function is calculated with the particle in a cell method combined with an *ab initio* tight-binding model to compute the total energy of wanderer displacement (Cohen et al. 1994). First principles all electron calculations, using the linearized augmented plane wave (LAPW) method, were used to compute the static total energy and the contribution due to the thermal excitations of electrons. In this study, the vibrational partition function was written in the form (Eqn. 1), that is, the total energy rather than the electronic free energy appears in the integrand. Since iron is a metal this is an approximation and corresponds to the neglect of the coupling between electronic and phonon excitations. Subsequent calculations show that this approximation is not a serious source of error for iron (Steinle-Neumann et al. 2000). The supercell contains 108 atoms and the Brillouin zone is sampled at a single k-point (the Γ-point at the zone center).

Monte Carlo method. This method was the first to be applied to the study of many-atom condensed matter systems (Metropolis et al. 1953) (see also chapters by Cygan and

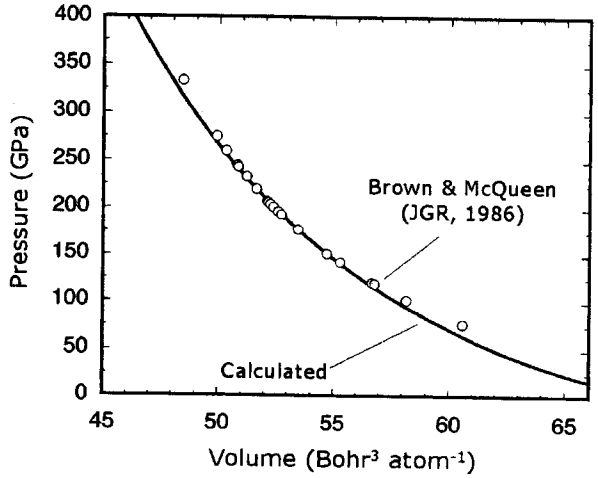

Figure 4. Results of a study of close-packed iron based on the particle in a cell method (Wasserman et al. 1996b). Theoretical and experimental (Brown and McQueen 1986) Hugoniots are in excellent agreement. The temperature along the Hugoniot increases with increasing pressure (not shown). The theoretical results predict a temperature of 5600 K at 243 GPa in excellent agreement with some experimental determinations (Brown and McQueen 1986) and approximately 1000 K lower than the results of Yoo et al. (1993).

Kalinichev, this volume). The Monte Carlo method does not suffer the approximations of the particle in a cell method; atoms are not restricted to be near their ideal lattice sites, and correlation between atomic motion is taken into account. This means that the Monte Carlo method is equally applicable to all states of matter: solid, liquid, or gas. On the other hand, the Monte Carlo method (and molecular dynamics), as it is most commonly applied, has the disadvantage of not computing the partition function directly, although special techniques for this have been developed. In most typical applications, one calculates instead ensemble averages of those thermodynamic properties that are defined for individual configurations (snapshots) of the system. These properties include the internal energy and the pressure, for example, but not the entropy or free energy. For any thermodynamic property that is defined for each configuration of the system X, the ensemble average is

$$\langle X \rangle = \frac{\int X(\mathbf{R}_1, \mathbf{R}_2, ...\mathbf{R}_N) \exp\left[-E(\mathbf{R}_1, \mathbf{R}_2, ...\mathbf{R}_N)/kT\right] d\mathbf{R}_1 d\mathbf{R}_2 ... d\mathbf{R}_N}{Z} \quad (10)$$

where $Z = QN!\Lambda^{3N}$ is the configuration integral. For the calculation to be efficient, we bias our sampling of configuration space towards those regions that contribute most to the integral, that is towards configurations that have relatively low energy. We must then remove this bias when computing the ensemble average. If the probability of the existence of a certain configuration m in our sample be $W(m)$, then, replacing integrals by sums

$$\langle X \rangle \approx \frac{\sum_m X(m) \exp\left[-E(m)/kT\right]/W(m)}{\sum_m \exp\left[-E(m)/kT\right]/W(m)} \quad (11)$$

where the specification of the configuration is denoted symbolically by m. A natural choice for $W(m)$ is the Boltzmann distribution, $W(m)=\exp[-E(m)/kT]$. In this case, the calculation of the ensemble average reduces to a simple, unweighted average over configurations

$$\langle X \rangle \approx \frac{1}{M}\sum_{m=1}^{M} X(m) \tag{12}$$

where M is the total number of configurations. The generation of a biased sampling of configuration space is an example of importance sampling. Methods for producing a sample drawn from the Boltzmann distribution include the construction of a Markov chain in which the next configuration is generated from the previous one by moving one atom a small random amount (Wood and Parker 1957). The new configuration is accepted always if it lowers the total energy, and conditionally if the energy is increased: if a random number chosen on (0,1) is less than $\exp(-\Delta E/kT)$ where ΔE is the change in energy. Sampling is discussed in more detail in a number of references (Allen and Tildesley 1989; Frenkel and Smit 1996; Hansen and McDonald 1986).

A practical concern in any method of computational statistical mechanics is the choice of boundary conditions. In principle, in order to reproduce a macroscopic crystal, we would need to include a large number atoms in our simulation: $O(10^{12})$ for a volume of ~1 μm^3. Even with the efficiency gained by importance sampling, this would be an impossible task for a simulation in which the energy is calculated from first principles. However, such large systems are unnecessary. As in the case of the particle in a cell method, periodic boundary conditions based on a supercell are generally used. The effect on thermodynamic properties of correlation of atomic motions decays rapidly with increasing distance; convergence tests demonstrate that supercells containing of order 100 atoms accurately reproduce infinite system behavior. Another practical concern is the number of configurations that must be generated in order to adequately sample configuration space. This depends on the system; whereas fewer than 10^5 configurations may be sufficient for low density fluid systems (Wood and Parker 1957), as many as 2 million are required to obtain precise averages for silica glass (Stixrude and Bukowinski 1991). Depending on how many configurations are required, the Monte Carlo method may be more efficient for the computation of thermodynamic properties than the molecular dynamics method to be discussed next. The reason is that only the internal energy need be computed for each configuration. In contrast, molecular dynamics requires the computation of interatomic forces which may be substantially more costly. However, this disadvantage of molecular dynamics is often outweighed by the additional insight gained by computing the dynamics of the system directly.

Molecular dynamics. The methods described so far rely on ensemble averages to compute thermodynamic properties, that is averages over large numbers of possible configurations of the system. In contrast, the molecular dynamics method, first described for the case of continuous potentials by Rahman (1964), explore the time evolution of a single realization (see also chapters in this volume by Cygan and Garofalini). The foundation of the molecular dynamics method is the ergodic hypothesis. For a property X defined for each configuration (which we now abbreviate as $\mathbf{R}^N$) and each instant of time t

$$\langle X \rangle = \frac{\int X(\mathbf{R}^N)\exp\left[-E(\mathbf{R}^N)/kT\right]d\mathbf{R}^N}{Z} = \lim_{t\to\infty}\frac{1}{t}\int_0^t X(t)dt \tag{13}$$

That is, given sufficient duration, time averages are equivalent to ensemble averages.

Molecular dynamics closely mimics the experimental situation where measurements of thermodynamic properties also generally rely on the ergodic hypothesis.

The essence of the molecular dynamics method is a straightforward application of Newton's second law. To obtain the time evolution of the system, we integrate the set of coupled second order differential equations

$$\begin{aligned}
\ddot{\mathbf{R}}_1 &= \mathbf{F}_1(\mathbf{R}_1,\mathbf{R}_2,\ldots,\mathbf{R}_N)/m_1 \\
\ddot{\mathbf{R}}_2 &= \mathbf{F}_2(\mathbf{R}_1,\mathbf{R}_2,\ldots,\mathbf{R}_N)/m_2 \\
&\vdots \\
\ddot{\mathbf{R}}_N &= \mathbf{F}_N(\mathbf{R}_1,\mathbf{R}_2,\ldots,\mathbf{R}_N)/m_N
\end{aligned} \tag{14}$$

where dots indicate time derivatives, $\mathbf{F}_i$ is the force acting on nucleus i, m_i is the nuclear mass, and the dependence of the force on the positions of all other nuclei is made explicit. The force may be calculated by any of the methods discussed in the section on "Total energy, forces, and stresses." It is the calculation of the force that determines the physics, assuming that all practical issues have been controlled (see below). It is important to realize that the simulation itself is simply a method for solving efficiently the differential equations and does not add any physical content. So for example, if the forces are calculated by density functional theory, the choice of the exchange-correlation potential (e.g., LDA or GGA) will completely determine the outcome of the simulation in terms of average thermodynamic or dynamic quantities.

Periodic boundary conditions are generally chosen for the solution of the differential equations. As for other statistical mechanical methods, a supercell of ~100 atoms is often sufficient for the computation of equilibrium thermodynamic properties. The choice of initial conditions is in principle irrelevant. Given a molecular dynamics trajectory of infinite duration, the system will evolve towards the equilibrium structure regardless of the initial arrangement. In practice, the trajectory is of finite duration and the system may not be able to transform to the equilibrium structure within the allotted time. This situation is also encountered in experiments where kinetics may hinder the formation of the equilibrium phase over finite time scales. As in experiments, the approach to equilibrium may be speeded in molecular dynamics simulations by increasing the temperature of the system. The initial conditions consist of a specification of the positions and velocities of the nuclei. The velocities are generally drawn pseudo-randomly from a Gaussian (Maxwell) distribution that corresponds to the temperature of interest. Other practical issues include the choice of method used to integrate the differential equations numerically, and the choice of the appropriate time step (Allen and Tildesley 1989).

Because Newton's equations of motion are conservative, the natural ensemble is *NVE* (micro-canonical), that is one in which the internal energy rather than the temperature is held constant. This is inconvenient if one wishes to compare with experiment where it is the temperature that is generally controlled. In order to perform molecular dynamics in the canonical ensemble, a thermostat must be applied to the system. This is accomplished by constructing a pseudo-Lagrangian. Many forms for temperature-conserving Lagrangians have been proposed, most of which can be written in a form that adds a frictional (velocity-dependent) term to the equations of motion (Allen and Tildesley 1989). Physically, the thermostat can be thought of as a heat bath to which the system is coupled. In the *NPT* ensemble, in which the pressure is held constant, the cell size and shape fluctuates. The choice of dynamical variables is critical. If the lattice parameters are chosen as in the method of Parrinello and Rahman (1981), the time evolution may depend on the chosen size or shape of the supercell. This difficulty is

liminated by a re-formulation in which the components of the strain tensor are cast as the lynamical variables (Wentzcovitch 1991).

As an example of the application of molecular dynamics, we show a study of liquid ron using an *ab initio* tight-binding model (Stixrude et al. 1998; Wasserman et al. 1996a) Fig. 5). Simulations were run in the *NVT* ensemble with the thermostat of Berendsen et al. (1984). The supercell contained 108 atoms, and the simulation was run with a timestep of 1 fs for approximately 1 ps. Conditions were chosen to be typical of the Earth's outer core. The structure of liquid iron is represented by the radial distribution function, $g(r)$, which describes the probability of finding pairs of nuclei separated by a distance r; the function is normalized to unity for a random distribution (McQuarrie 1976). The results show the excluded volume about each nucleus, due to repulsion at short distances, the strong first peak due to first nearest neighbors in the liquid, and the weakening of positional correlation at larger distances. The structure is more pronounced at lower temperatures, where the potential energy of interaction is larger as compared with the kinetic energy.

SELECTED APPLICATIONS

Overview

We show two examples of the combination of statistical mechanics with first principles electronic structure methods. Although first principles molecular dynamics has been applied for some time to the study of relatively simple systems, its application to Earth materials is more recent. These examples illustrate the power of modern density functional theory and the ability that now exists to treat large systems at high temperature.

Phase transformations in silicates

The common minerals of the Earth's upper mantle are known all to undergo a series of phase transformations with increasing pressure. Because these transformations entail a change in physical properties, they are manifest in the structure of the earth's interior,

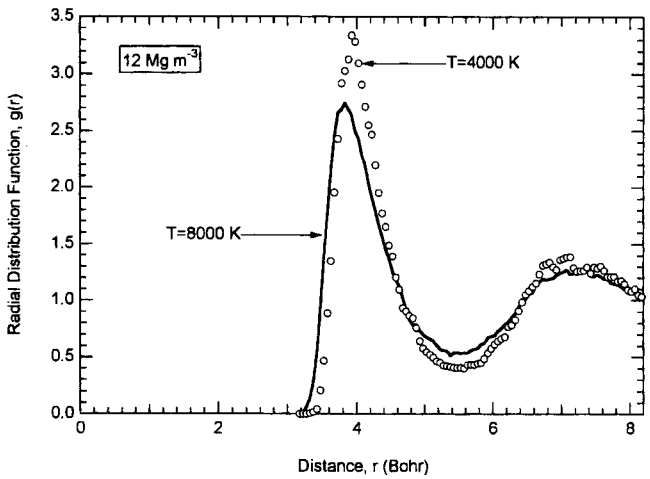

Figure 5. Radial distribution function of liquid iron at a density typical of that of the Earth's outer core (Wasserman et al. 1996a). Results are from molecular dynamics simulations based on an ab initio tight-binding model (Cohen et al. 1994).

most notably in discontinuities in seismic wave velocities and density, for example, at 410 and 660 km depth (Jeanloz and Thompson 1983). Of particular interest to geophysics is the discovery of new phase transitions that may exist at pressure-temperature conditions beyond the current reach of experimental methods. For example, our picture of the earth's interior was profoundly altered by the discovery (Liu 1975) that common minerals of the upper mantle transform at high pressure to assemblages dominated by an Mg-rich metasilicate with the perovskite structure. It is now widely accepted that perovskite is the most abundant mineral in the earth's lower mantle (Bukowinski and Wolf 1990; Karki and Stixrude 1999; Knittle and Jeanloz 1987; Stixrude et al. 1992; Wang et al. 1994).

Over the range of pressure and temperature so far explored in the laboratory, the observed structure of $(Mg,Fe)SiO_3$ perovskite is orthorhombic Pbnm (Horiuchi et al. 1987). However, because experiments have not yet accessed the entire pressure-temperature range spanned by the lower mantle, there has for some time been speculation that the structure of this phase at lower mantle conditions may differ from that experimentally observed. The perovskite structure is remarkably rich and accommodates a large variety of polymorphs, which are related by rotations of the SiO_6 octahedra about the three pseudo-cubic axes (Glazer 1972; Glazer 1975) (Fig. 6). Thus Pbnm may be classified as $(--+)$. Initial work was based on *ab initio* models and focused on higher symmetry polymorphs that result from un-freezing (vanishing) of one or more octahedral rotations including $(00+)$, $(--0)$, (-00), and the cubic parent structure (000) (Wolf and Bukowinski 1987). However, subsequent first principles calculations showed that the enthalpies of these structures were much higher than that of Pbnm and that their stabilization at temperatures below melting was unlikely (Stixrude and Cohen 1993).

In order to investigate the structure of $MgSiO_3$ perovskite at lower mantle conditions, Kiefer and Stixrude (2001) performed first principles molecular dynamics simulations. The calculations are based on density functional theory within the local density approximation. For these plane-wave pseudopotential calculations we used the Vienna *Ab initio* Simulation Package (VASP) (Kresse and Furthmüller 1996a; Kresse and Furthmüller 1996b; Kresse and Hafner 1993). The simulation supercell contains 80 atoms, or four primitive unit cells of the Pbnm structure. Convergence tests with a rigid ion pair potential showed that pressures calculated with this supercell differed from the infinite system result by less than 1%. The initial condition was chosen as the equilibrium

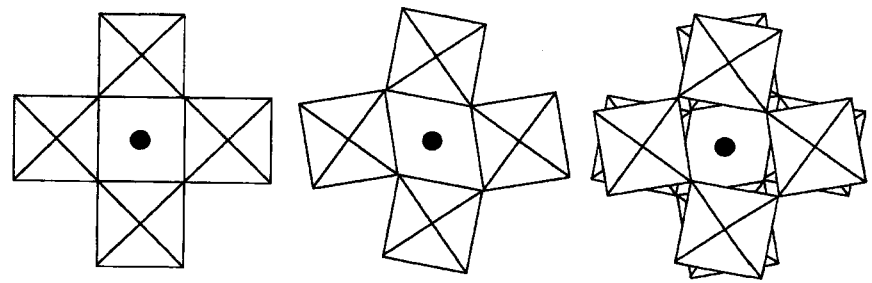

Figure 6. Octahedral rotations in the perovskite structure. The left figure shows the structure of the parent cubic structure viewed along one of the cubic axes. The other figures show structures in which the octahedra rotate rigidly. In the middle figure, the sense of rotation is identical in all octahedral planes normal to the rotation axis. This is an example of a (+) type rotation in the notation of Glazer (1972). The right figure illustrates a (–) type rotation in which alternating planes rotate in opposite directions.

bnm structure under static conditions. Simulations were performed in the canonical nsemble (fixed temperature and cell shape and size); temperature was maintained with a losé (1984) thermostat. The time step was 1 fs, and the simulations were run for 1.6 ps.

The results of one simulation are shown in Figure 7. The density (5184 kg m^{-3}) and :mperature (2000 K), correspond to conditions typical of the mid-lower mantle Dziewonski and Anderson 1981). In the first half of the simulation, the stress is nearly otropic and fluctuates about a mean value of 82 GPa. This is 9 GPa larger than the alculated static pressure in excellent agreement with the experimentally determined ermal pressure (Fiquet et al. 2000). The fact that the stress remains isotropic upon pplication of temperature means that the thermal expansivity of the Pbnm phase is pproximately isotropic, in agreement with experimental results (Fiquet et al. 2000; unamori et al. 1996). After 0.7 ps, the character of the stress tensor changes rapidly and pproaches a new stable configuration. The mean stress (pressure) increases by 6% to 87 iPa, and the stress becomes anisotropic. In order to investigate the origin of this change, ie simulated structure was examined in detail.

The change in stress state between 0.7 ps and 0.8 ps is caused by a change in the tructure of the material. The transformation consists of a homogeneous rotation of half ie SiO_6 octahedra that persists for the remainder of the simulation (Fig. 8). The new tructure has a (−++) pattern of octahedral rotation which corresponds to Pmmn ymmetry. The change with respect to the Pbnm phase is more subtle than phase ansformations that had been contemplated in previous theoretical and experimental ork: none of the three octahedral rotations vanish in the Pmmn structure and the agnitude of the octahedral rotations is similar to that in Pbnm. The increase in mean tress at the transition means that the Pmmn phase has a slightly larger volume than Pbnm t the same pressure. The anisotropy of the stress tensor reflects the differences in quilibrium axial ratios between the two phases.

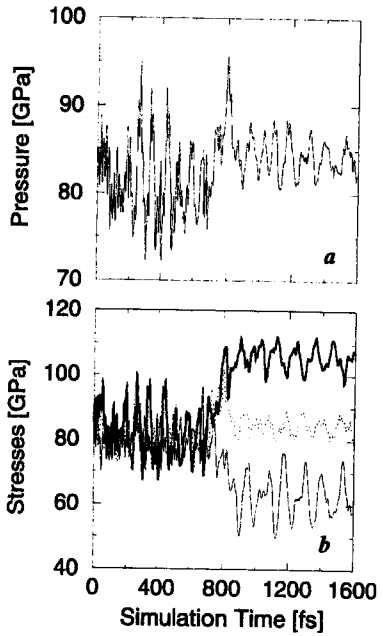

Figure 7. Results of first principles molecular dynamics simulation of $MgSiO_3$ perovskite at a density of 5184 kg m^{-3} and a temperature of 2000 K including a) pressure and b) the longitudinal components of the stress tensor: (bold) σ_{11}, (light) σ_{22}, (dashed) σ_{33}. The off-diagonal components of the stress tensor do not differ significantly from zero.

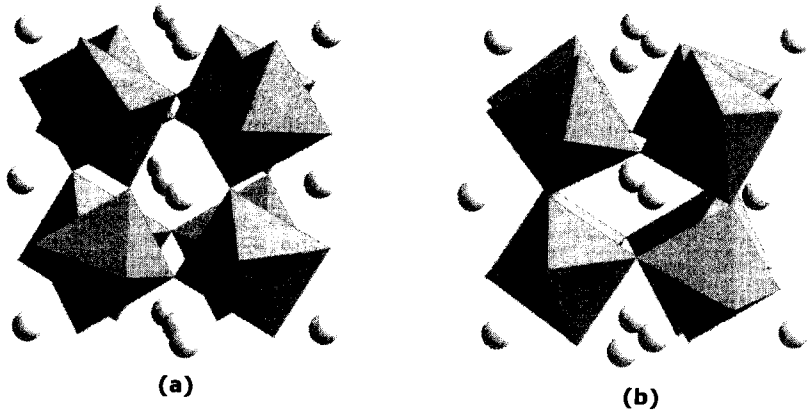

Figure 8. Two snapshots of a portion of the simulation cell taken from first principles molecular dynamics simulations of $MgSiO_3$ perovskite at a) 0 ps and b) 0.79 ps. The view is along [110] of the Pbnm phase.

In order to further investigate the properties of the new phase and the phase transition, we performed a series of static calculations. The Pbnm phase is found to be lower in energy than the Pmmn phase by 0.085 eV/atom at static conditions, a difference that significantly exceeds the typical numerical precision of these calculations (1 meV/atom). While the magnitude of the difference is likely to be underestimated (see below) this result is consistent with earlier all electron calculations that found Pbnm to be the ground state (Stixrude and Cohen 1993). The static energy difference is comparable to the available thermal energy in our molecular dynamics simulation, supporting the occurrence of Pmmn as an equilibrium phase at high temperature. Since the Pmmn phase is stabilized by increasing temperature, it must have a higher entropy than the Pbnm phase. The new Pmmn phase has a larger volume than Pbnm as evidenced by the increase in pressure at the transition in our constant volume simulations. Since the volume and entropy of transition have the same sign, the Clapeyron slope must be positive.

In order to test the robustness of our conclusions, we performed static all-electron calculations of the total energy of the two phases using the linearized augmented plane wave (LAPW) method (Singh 1994). The all-electron calculations show that difference in energy between Pbnm and Pmmn is 0.132 eV/atom, or approximately 50% more than the pseudopotential result. Because the pseudopotential calculations underestimate the energy difference, it is likely that our molecular dynamics simulations underestimate the temperature at which the Pmmn phase becomes stable. We infer that the transition temperature between Pbnm and Pmmn phases may be somewhat greater than in our molecular dynamics simulations, and may be as high as 3000 K, based on the magnitude of the pseudopotential error. A transition temperature significantly higher than 2000 K would be consistent with experimental results which show that the Pbnm phase is stable to 2000 K at 30 GPa and 90 GPa (Fiquet et al. 2000; Funamori et al. 1996).

The location of the phase transition is similar to the conditions of pressure and temperature expected in the Earth's lower mantle. When one takes into account the likely magnitude of lateral variations in temperature (several hundred K), we find that a phase transformation from Pbnm to Pmmn may occur in the hotter portions of the mantle over a range of depths spanning several hundred km. Although the change in structure at the predicted Pbnm to Pmmn phase transition is subtle, changes in physical properties may be geophysically significant. We have calculated the full elastic constant tensor of both

phases at static conditions. The results show that the Pmmn has a higher bulk sound velocity that Pbnm, but a lower shear wave velocity. If this transition occurs in the lower mantle, it would have an unusual seismological signature, one in which the thermally-induced change in bulk and shear wave velocities are anti-correlated. Such anti-correlation is seen in some models of seismic tomography, especially beneath the Pacific in the deep lower mantle (Masters et al. 2000) which is found to be anomalously slow in S-wave velocity, but fast in bulk sound velocity. The predicted phase transition may provide an explanation of these seismic observations.

Very recently another group has performed first principles molecular dynamics simulations of $MgSiO_3$ perovskite using methods similar to ours (Oganov et al. 2001). This group finds that the Pbnm phase is stable throughout the pressure-temperature regime of their study, which overlaps the conditions at which we find a phase transformation. The reason for this discrepancy is not clear, but may be related to differences in pseudopotential construction, run time, initial conditions, or other factors.

High temperature properties of transition metals

Transition metals are particularly challenging because of the localized nature of the d-electrons. To accurately represent these valence states requires large plane-wave basis sets. Moreover, reciprocal space must be sampled densely in order to capture the positions of bands with respect to the Fermi level. These special properties make total energy calculations of transition metals costly. Geophysically the most important transition metal is iron, which makes up most of the earth's core (see Jeanloz 1990 and references therein for a review). Recently, there have been considerable advances in the theoretical study of liquid and solid iron and its alloys at the pressure temperature conditions of the earth's core. In a pioneering study de Wijs et al. (1998) used first principles molecular dynamics to predict the viscosity of liquid iron at conditions of the earth's core. The properties of the liquid state were further studied by Alfé et al. (2000b). The thermodynamics of solid iron, in its hexagonal phase, was investigated by Alfé et al. (1999b) by combining density functional theory with lattice dynamics and an approximate correction for anharmonic effects. Studies of solid and liquid have been combined to predict the melting curve of pure iron (Alfé et al. 1999a). More recently, the properties of iron alloys have also been examined (Alfé et al. 2000a).

Because much of our knowledge of the earth's interior comes from seismology, an understanding of the elastic properties of earth materials is particularly important to geophysics. The elastic constants of solid iron are of special interest because of the unusual seismic properties of the earth's inner core. Among these are its high Poisson ratio (0.44) which is nearly that of a liquid (0.5) and its anisotropy: compressional waves travel approximately 3% faster along the polar axis than in the equatorial plane (Creager 1992; Tromp 1993). Subsequent studies have shown that the anisotropy may be heterogeneous on length scales ranging from a few km to a few thousand km (Creager 1997; Tanaka and Hamaguchi 1997; Vidale et al. 2000) and that the anisotropy may change with time, a result that was interpreted in terms of super-rotation of the inner core (Song and Richards 1996; Su et al. 1996).

The elastic constants of iron have been studied experimentally and theoretically at low temperature and high pressure (Mao et al. 1998; Söderlind et al. 1996; Steinle-Neumann et al. 1999; Stixrude and Cohen 1995), but there has not yet been a first principles calculation of the full elastic constant tensor at inner core conditions (see Nye 1985 for a review of elastic constants). Laio et al. (2000) developed a clever hybrid method that combines first principles total energy and force calculations for a limited number of time steps with a semi-empirical potential fit to the first principles results. These authors investigated a number of properties with their *ab initio* method including

the melting curve, and the Poisson ratio of iron at inner core conditions, which they find to be similar to that seismologically observed.

In order to investigate the full elastic constant tensor of iron at inner core conditions, Steinle-Neumann et al. (2001) combined first principles GGA density functional theory with the particle in a cell method. The crystallographic structure of iron was assumed to be hexagonal close-packed (hcp). Experiments show that this is the low temperature high pressure phase of iron from 10 GPa, to at least 300 GPa, the highest pressures so far explored in static experiments (Mao et al. 1990). Experiments also show that hcp is the liquidus phase to at least 100 GPa (Shen et al. 1998). There is theoretical evidence that hcp is the stable phase of iron at the conditions of the Earth's inner core (Vocadlo et al. 1999). Experimental observations of other structures at high pressures and temperatures (Andrault et al. 1997; Saxena et al. 1995) have been controversial (Boehler 2000); the proposed structures are closely related to hcp.

Because the axial ratio c/a of hcp iron is observed experimentally to vary significantly with pressure and temperature, we were careful to determine the minimum energy structure of this phase at all conditions. The results (Fig. 9) show that the axial ratio of hcp iron at conditions comparable to those in the inner core (~1.7) is significantly greater than that found at low temperatures in experiment and theory (~1.6) (Jephcoat et al. 1986; Mao et al. 1990; Stixrude et al. 1994). Our results are consistent with experiments at lower pressures (Funamori et al. 1996; Huang et al. 1987), and earlier theoretical work that also found that c/a increases with temperature (Wasserman et al. 1996b).

The temperature induced increase in the axial ratio has important implications for the elasticity of iron (Fig. 10). We determined the elastic constants by calculating the change in the Helmholtz free energy upon application of small amplitude finite strains, chosen to constrain the five independent components of the elastic constant tensor of this hexagonal material (Steinle-Neumann et al. 1999). The results show that the relative magnitude of the two longitudinal moduli, c_{33} and c_{11}, changes as the temperature increases. Whereas previous theoretical calculations (Stixrude and Cohen 1995) and experiments (Mao et al. 1998) have found $c_{33} > c_{11}$ at low temperatures, our results show that $c_{33} < c_{11}$ at high temperatures. The origin of this effect is the increase in the axial ratio. As the c-axis expands, it becomes more compressible, thereby lowering c_{33} relative to c_{11}. Other elastic moduli also change in relative magnitude; the off-diagonal modulus c_{12} increases rapidly with temperature, becoming nearly equal to c_{11} at the highest temperatures investigated. This behavior also has its origin in the temperature-induced increase of c/a and the contraction of the basal plane that it entails. The two shear moduli, c_{44} and $c_{66}=1/2(c_{11}-c_{12})$ decrease by nearly a factor of four from 0 K to 6000 K.

The behavior of the elastic moduli has important implications for our understanding of the shear elasticity of Earth's inner core. The very high Poisson's ratio of the inner core has been interpreted as requiring anomalous dispersion and the presence of partial melt (Singh et al. 2000). Instead, we find that the high Poisson ratio of the inner core results from the effects of high pressure and temperature on the elasticity of iron. The predicted adiabatic bulk and shear moduli of iron agree well with those of the inner core at a temperature of 5700 K. The calculated Poisson's ratio at 5700 K (0.44) is in excellent agreement with previous theoretical estimates (Laio et al. 2000), and with the seismologically determined value for the inner core.

As the inner core is nearly isothermal (Stixrude et al. 1997), the comparison of the elastic properties of iron with those of the inner core determined seismologically provides a way to estimate the temperature in the earth's deep interior. This approach is

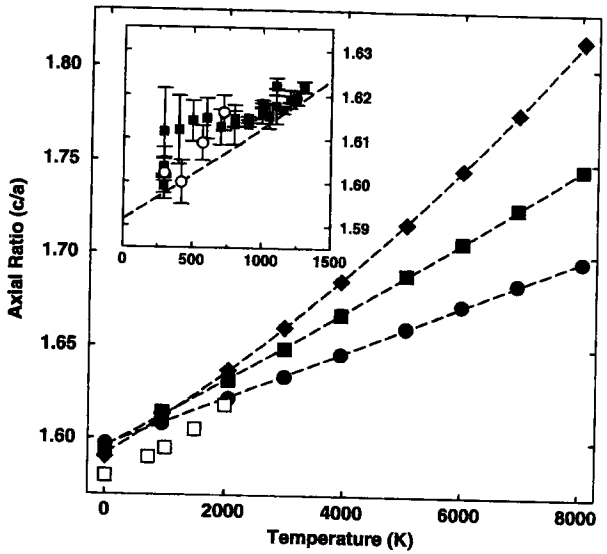

Figure 9. Predicted structure of hcp iron from particle in a cell method with first principles calculations of the energetics (dark symbols) at densities of (diamonds) 12.52 Mg m^{-3} (squares) 13.04 Mg m^{-3} (circles) 13.62 Mg m^{-3}. Results are compared with earlier theoretical predictions based on more approximate ab initio calculations of the total energy (open squares) (Wasserman et al. 1996b) and (inset) with a polybaric set of experimental results at lower pressure from (open circles) (Huang et al. 1987) (15-20 GPa) and (squares) (Funamori et al. 1996) (23-35 GPa).

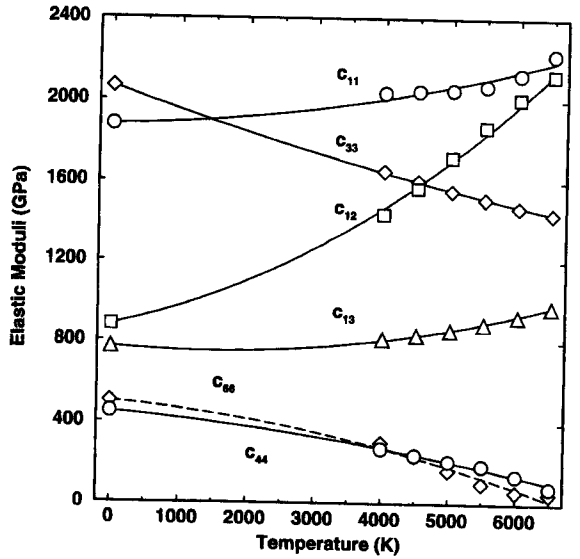

Figure 10. Elastic constants of hcp iron at a density of 13 Mg m^{-3}, typical of that in the Earth's inner core, from first principles particle in a cell method calculations. There are five independent elastic constants in a hexagonal material. Results for $c_{66}=1/2(c_{11}-c_{12})$ are shown for comparison with the other shear modulus c_{44}.

complementary to estimates based on the melting temperature of iron which suffer uncertainty due to the unknown but possibly large influence of light alloying elements (see Jeanloz 1990 for a review). Assuming a melting point depression of a few hundred degrees, our value for inner core temperature (5700 K) is consistent with estimates of the melting point of pure iron at the inner core boundary by Alfé et al. (1999a) (6400 K) and those based on extrapolation of the melting point on the Hugoniot (~6000 K) (Brown and McQueen 1986). The theoretical result of Laio et al. (2000) (5400 K) and the extrapolated melting curve from static experiments (~5000 K) both fall below our estimate.

The ratio of the longitudinal moduli c_{33}/c_{11} controls the sense of the P-wave anisotropy of the single crystal. The new results show that the sense of this anisotropy at high temperature is opposite to what had been found at lower temperatures in experiment and theory (Mao et al. 1998; Stixrude and Cohen 1995). At high temperature, P-waves propagate 12.5% faster in the basal plane than along the c-axis. This means that, in order to explain the anisotropy of the polycrystalline inner core, the basal planes of the constituent crystals must be preferentially aligned with the Earth's rotation axis. We have shown that a simplified textural model, in which the basal planes are all parallel to the rotation axis, and in which crystals are otherwise randomly oriented, explains well the pattern of anisotropy in the Earth's inner core. Further progress in understanding the origin of inner core anisotropy will require advances in two areas: 1) the origin of the macroscopic stress field that must be responsible for producing the texture and 2) the microscopic mechanisms by which this stress field produces the preferred orientation.

CONCLUSIONS AND OUTLOOK

It is now possible to explore the high temperature properties of Earth materials from first principles. The combination of efficient first principles methods for computing the total energy, interatomic forces, and stresses, with a variety of statistical mechanical methods including molecular dynamics, Monte Carlo, and approximate treatments such as the cell model promises rapid progress. With continued advances in computational power, and in the development of new theoretical methods, one foresees significant progress in three areas.

Scale

The equilibrium properties of many pure phases, even those with large unit cells such as $MgSiO_3$ perovskite can now be explored with supercells of manageable size. What is not yet possible is the first principles exploration of high temperature phenomena and materials that possess inherently long length scales. Examples include those systems involving imperfect crystals. These are important for understanding a host of phenomena including element partitioning, diffusion, deformation mechanisms, and the interaction with light. From the theoretical point of view, the size of the system (supercell) that must be constructed is proportional to the inverse of the abundance of the rarest constituent. The study of the behavior of impurities or defects in the dilute limit, of interest in a wide variety of geological applications may require very large supercells. Dislocations are large imperfections in the lattice that may require systems of thousands of atoms. The study of their dynamics may require the combination of first principles methods with more advanced statistical mechanical techniques such as non-equilibrium molecular dynamics (Hoover 1983), something which has not yet been attempted.

Duration

Many phenomena have inherently long time scales. Examples include the kinetics of phase transformations, and the deformation of high viscosity materials including many

ilicate liquids. The study of the deformation of solid silicates in the Earth's interior may ncompass the largest range of time scales in any natural system: from that of atomic ibration to that of mantle convection. The study of these systems by molecular dynamics s challenging because the time step must be short enough to capture the fastest degrees of reedom, and the number of time steps great enough to sample the slowest. To overcome his problem, multi-time step (Swindoll and Haile 1984), generalized Langevin Romiszowski and Yaris 1991), and other methods (Sørensen and Voter 2000) have been leveloped which may be applicable to Earth systems although these have not yet been ısed in conjunction with first principles electronic structure methods.

Materials

Current approximations to density functional theory are not equally successful for all naterials. While its formulation is general, there are some materials for which the LDA ınd GGA do not seem to be adequate. Examples include the transition metal oxides, and presumably transition metal bearing silicates as well. The problem is that the strongly localized Coulomb repulsion between d electrons does not seem to be adequately represented. As a consequence, FeO wüstite is predicted to be a metal in LDA and GGA, whereas experimental observations find an insulator. Despite this failure, it is interesting to note that the structural and elastic properties of FeO are well reproduced by LDA (Isaak et al. 1993). In any case, the complete understanding of Mott insulators will require new advances in theory. These will need to go beyond such developments as the LDA+U method which has yielded considerable insight but adds the local Coulomb repulsion (U parameter) in an ad hoc manner (Mazin and Anisimov 1997).

ACKNOWLEDGMENTS

This work supported by the National Science Foundation under grant EAR-9973139.

REFERENCES

Alfé D, Gillan MJ, Price GD (1999a) The melting curve of iron at pressures of the earth's core from *ab initio* calculations. Nature 401:462-464
Alfé D, Gillan MJ, Price GD (2000a) Constraints on the composition of the earth's core from *ab initio* calculations. Nature 405:172-175
Alfé D, Kresse G, Gillan MJ (2000b) Structure and dynamics of liquid iron under earth's core conditions. Phys Rev B 61:132-142
Alfé D, Price GD, Gillan MG (1999b) Thermodynamics of hexagonal-close-packed iron under earth's core conditions. Physical Review B: submitted
Allen MP, Tildesley DJ (1989) Computer Simulation of Liquids. Clarendon Press, Oxford
Andrault D, Fiquet G, Haydock R (1997) The orthorhombic structure of iron: An *in situ* study at high-temperature and high-pressure. Science 278:831-834
Berendsen HJC, Postma JPM, Gunsteren WFV, Nola AD, Haak JR (1984) Molecular dynamics with coupling to an external bath. J Chem Phys 81:3684-3690
Boehler R (2000) High-pressure experiments and the phase diagram of lower mantle and core materials. Rev Geophys 38:221-245
Born M, Huang K (1954) Dynamical Theory of Crystal Lattices. Clarendon Press, Oxford
Brown JM, McQueen RG (1986) Phase transitions, Grüneisen parameter, and elasticity for shocked iron between 77 GPa and 400 GPa. J Geophys Res 91:7485-7494
Bukowinski MST, Wolf GH (1990) Thermodynamically consistent decompression—implications for lower mantle composition. J Geophys Res 95:12583-12593
Callen HB (1960) Thermodynamics. John Wiley and Sons, New York
Car R, Parrinello M (1985) Unified approach for molecular dynamics and density-functional theory. Phys Rev Let 55:2471-2474
Cohen ML, Heine V (1970) The fitting of pseudopotentials to experimental data and their subsequent application. Sol State Phys 24:38-249

Cohen RE, Mehl MJ, Papaconstantopoulos DA (1994) Tight-binding total-energy method for transition and noble metals. Phys Rev B 50:14694-14697
Cowley ER, Gong Z, Horton GK (1990) Theoretical study of the elastic and thermodynamic properties of sodium chloride under pressure. Phys Rev B 41:2150-2157
Creager KC (1992) Aninsotropy of the inner core from differential travel times of the phases PKP and PKIKP. Nature 356:309-314
Creager KC (1997) Inner core rotation rate from small-scale heterogeneity and time-varying travel times. Science 278:1284-1288
Davies GF (1999) Dynamic Earth: Plates, Plumes, and Mantle Convection. Cambridge University Press, Cambridge
Dove MT (1993) Introduction to Lattice Dynamics. Cambridge University Press, Cambridge
Dziewonski AM, Anderson DL (1981) Preliminary reference earth model. Phys Earth Planet Int 25:297-356
Dziewonski AM, Gilbert JF (1971) Solidity of the inner core of the earth inferred from normal mode observations. Nature 234:465-466
Feynman RP (1939) Forces in molecules. Phys Rev 56:340-343
Fiquet G, Dewaele A, Andrault D, Kunz M, Bihan TL (2000) Thermoelastic properties and crystal structure of $MgSiO_3$ perovskite at lower mantle pressure and temperature conditions. Geophys Res Let 27:21-24
Frenkel D, Smit B (1996) Understanding Molecular Simulation: from Algorithms to Applications. Academic Press, San Diego
Funamori N, Yagi T, Uchida T (1996) High-pressure and high-temperature in situ x-ray diffraction study of iron to above 30 GPa using MA8-type apparatus. Geophys Res Let 23:953-956
Glazer AM (1972) Classification of tilted octahedra in perovskites. Acta Crystal B 28:3384-&
Glazer AM (1975) Simple ways of determining perovskite structures. Acta Crystal A 31:756-762
Gordon RG, Kim YS (1972) Theory for the forces between closed-shell atoms and molecules. J.Chem.Phys. 56:3122-3133
Hansen JP, McDonald IR (1986) Theory of Simple Liquids. Academic Press, London
Heine V (1970) The pseudopotential concept. Solid State Phys 24:1-37
Hellman H (1937) Einfuhrung in die Quantumchemie. Deuticke, Leipzig
Hill TL (1956) Statistical Mechanics: Principles and Selected Applications. McGraw-Hill, New York
Hohenberg P, Kohn W (1964) Inhomogeneous electron gas. Phys Rev B 136:864-871
Holt AC, Hoover WG, Gray SG, Shortle DR (1970) Comparison of the lattice-dynamics and cell-model approximations with Monte-Carlo thermodynamic properties. Physica 49:61-76
Hoover WG (1983) Non-equilibrium molecular-dynamics. Ann Rev Phys Chem 34:103-127
Horiuchi H, Ito E, Weidner DJ (1987) Perovskite-type $MgSiO_3$ single-crystal x-ray-diffraction study. Am Min 72:357-360
Huang E, Bassett WA, Tao P (1987) Pressure-temperature-volume relationship for hexagonal close packed iron determined by synchrotron radiation. J Geophys Res 92:8129-8135
Isaak DG, Cohen RE, Mehl MJ, Singh DJ (1993) Phase stability of wüstite at high-pressure from 1st-principles linearized augmented plane-wave calculations. Phys Rev B 47:7720-7731
Jeanloz R (1990) The nature of the earth's core. Ann Rev Earth Planet Sci 18:357-386
Jeanloz R, Thompson AB (1983) Phase transitions and mantle discontinuities. Rev Geophys 21:51-74
Jephcoat A, Mao HK, Bell PM (1986) Static compression of iron to 78 GPa with rare gas solids as pressure-transmitting media. J Geophys Res 91:4677-4686
Jones RO, Gunnarsson O (1989) The density functional formalism, its applications and prospects. Rev Mod Phys 61:689-746
Karki BB, Stixrude L (1999) Seismic velocities of major silicate and oxide phases of the lower mantle. J Geophys Res: in press
Kiefer B, Stixrude L (2001) Phase transition in $MgSiO_3$ perovskite. Nature: submitted
Kieffer SW (1979) Thermodyanamics and lattice vibrations of minerals, I: mineral heat capacities and their relationship to simple lattice vibrational modes. Rev Geophys Space Phys 17:1-19
Kittel C (1996) Introduction to solid state physics. Wiley, New York
Knittle E, Jeanloz R (1987) Synthesis and equation of state of $(Mg,Fe)SiO_3$ perovskite to over 100 gigapascals. Science 235:668-670
Kohn W, Sham LJ (1965) Self-consistent equations including exchange and correlation effects. Phys Rev A 140:1133-1138
Kresse G, Furthmüller J (1996a) Efficiency of ab-initio total energy calculations for metals and semiconductors using a plane-wave basis set. Comp Mat Sci 6:15-50
Kresse G, Furthmüller J (1996b) Efficient iterative schemes for *ab initio* total-energy calculations using a plane-wave basis set. Phys Rev B 54:11169-11186
Kresse G, Hafner J (1993) *Ab initio* molecular-dynamics for liquid-metals. Phys Rev B 47:558-561

Laio A, Bernard S, Chiarotti GL, Scandolo S, Tosatti E (2000) Physics of iron at earth's core conditions. Science 287:1027-1030
Landau LD, Lifshitz EM (1980) Statistical Physics. Pergamon, New York
Liu L (1975) Postoxide phases of forsterite and enstatite. Geophys Res Let 2:417-419
Lundqvist S, March NH (1987) Theory of the Inhomogeneous Electron Gas. Plenum Press, London
Mao HK et al. (1998) Elasticity and rheology of iron above 200 GPa and the nature of the earth's inner core. Nature 396:741-743
Mao HK, Wu Y, Chen LC, Shu JF, Jephcoat AP (1990) Static compression of iron to 300 GPa and $Fe_{0.8}Ni_{0.2}$ alloy to 260 GPa: Implications for composition of the core. J Geophys Res 95:21737-21742
Masters G, Laske G, Bolton H, Dziewonski A (2000) The relative behavior of shear velocity, bulk sound speed, and compressional velocity in the mantle: implications for chemical and thermal structure. *In:* Earth's Deep Interior: Mineral Physics and Tomography from the Atomic to the Global Scale. Karato S, Forte AM, Liebermann RC, Masters G, Stixrude L (eds). American Geophysical Union, Washington, DC, p 63-88
Mazin II, Anisimov VI (1997) Insulating gap in FeO: Correlations and covalency. Phys Rev B 55:12822-12825
McQuarrie DA (1976) Statistical Mechanics. Harper and Row, New York
Metropolis N, Rosenbluth AW, Rosenbluth MN, Teller AH, Teller E (1953) Equation of state calculations by fast computing machines. J Chem Phys 21:1087-1092
Nielsen OH, Martin R (1985) Quantum mechanical theory of stress and force. Phys Rev B 32:3780-3791
Nosé S (1984) A molecular-dynamics method for simulations in the canonical ensemble. Molec Phys 52:255-268
Nye JF (1985) Physical Properties of Crystals: Their Representation by Tensors and Matrices. Oxford, Oxford, UK
Oganov AR, Brodholt JP, Price GD (2001) *Ab initio* elasticity and thermal equation of state of $MgSiO_3$ perovskite. Earth Planet Sci Let 184:555-560
Parrinello M, Rahman A (1981) Polymorphic phase transitions in single-crystals—a new molecular dynamics method. J App Phys 52:7182-7290
Payne MC, Teter MP, Allan DC, Arias TA, Joanopoulos JD (1992) Iterative minimization techniques for *ab initio* total-energy calculations: molecular dynamics and conjugate gradients. Rev Mod Phys 64:1045-1097
Perdew JP, Burke K, Ernzerhof M (1996) Generalized gradient approximation made simple. Phys Rev Let 77:3865-3868
Pickett WE (1989) Pseudopotential methods in condensed matter applications. Comp Phys Rep 9:115-197
Rahman A (1964) Correlations in the motion of liquid argon. Phys Rev A 136:405-411
Reif F (1965) Statistical and Thermal Physics. McGraw-Hill, New York
Romiszowski P, Yaris R (1991) A dynamic simulation method suppressing uninteresting degrees of freedom. J Chem Phys 94:6751-6761
Saxena SK et al. (1995) Synchrotron x-ray study of iron at high-pressure and temperature. Science 269:1703-1704
Shen GY, Mao HK, Hemley RJ, Duffy TS, Rivers ML (1998) Melting and crystal structure of iron at high pressures and temperatures. Geophys Res Let 25:373-376
Singh DJ (1994) Planewaves, Pseudopotentials, and the LAPW Method. Kluwer Academic, Norwall, Massachusetts
Singh SC, Taylor MAJ, Montagner JP (2000) On the presence of liquid in earth's inner core. Science 287:2471-2474
Söderlind P, Moriarty JA, Willis JM (1996) First-principles theory of iron up to earth-core pressures: structural, vibrational, and elastic properties. Phys Rev B 53:14063-14072
Song X, Richards PG (1996) Seismological evidence for differential rotation of the Earth's inner core. Nature 382:221-224
Sørensen MR, Voter AF (2000) Temperature-accelerated dynamics for simulation of infrequent events. J Chem Phys 112:9599-9606
Stacey FD (1992) Physics of the Earth. Brookfield, Brisbane
Steinle-Neumann G, Stixrude L, Cohen RE (1999) First-principles elastic constants for the hcp transition metals Fe, Co, and Re at high pressure. Phys Rev B 60:791-799
Steinle-Neumann G, Stixrude L, Cohen RE, Gülseren O (2000) Elasticity of Iron at High Temperature and Pressure. Nature: submitted
Stevenson DJ (1987) Limits on lateral density and velocity variations in the earth's outer core. Geophys J Internat 88:311-319
Stixrude L, Bukowinski MST (1991) Atomic structure of SiO_2 glass and its response to pressure. Phys Rev B 44:2523-2534

Stixrude L, Cohen RE (1993) Stability of orthorhombic $MgSiO_3$-perovskite in the Earth's lower mantle Nature 364:613-616
Stixrude L, Cohen RE (1995) High pressure elasticity of iron and anisotropy of earth's inner core. Science 267:1972-1975
Stixrude L, Cohen RE, Hemley RJ (1998) Theory of minerals at high pressure. Reviews in Mineralogy 37:639-671
Stixrude L, Cohen RE, Singh DJ (1994) Iron at high pressure: linearized augmented plane wave calculations in the generalized gradient approximation. Phys Rev B 50:6442-6445
Stixrude L, Hemley RJ, Fei Y, Mao HK (1992) Thermoelasticity of silicate perovskite and magnesiowustite and stratification of the earth's mantle. Science 257:1099-1101
Stixrude L, Wasserman E, Cohen RE (1997) Composition and temperature of earth's inner core. J Geophys Res 102:24729-24739
Su W, Dziewonski AM, Jeanloz R (1996) Planet within a planet; rotation of the inner core of Earth. Science 274:1883-1887
Swindoll RD, Haile JM (1984) A multiple time step method for molecular dynamics simulations of fluids of chain molecules. J Comp Phys 53:298-298
Tanaka S, Hamaguchi H (1997) Degree one heterogeneity and hemispherical variation of anisotropy in the inner core from PKP(BC)-PKP(DF) times. J Geophys Res 102:2925-2938
Tromp J (1993) Support for anisotropy of the earth's core from free oscillations. Nature 366:678-681
Vidale JE, Dodge DA, Earle PS (2000) Slow differential rotation of the earth's inner core indicated by temporal changes in scattering. Nature 405:445-448
Vocadlo L, Brodholt J, Alfé D, Price GD, Gillan MJ (1999) The structure of iron under the conditions of the earth's inner core. Geophys Res Let 26:1231-2134
Wang YB, Weidner DJ, Liebermann RC, Zhao YS (1994) P-V-T equation of state of $(Mg,Fe)SiO_3$ perovskite - constraints on composition of the lower mantle. Phys Earth Planet Int 83:13-40
Wasserman E, Stixrude L, Cohen RE (1996a) Molecular dynamics simulations of liquid iron under outer core conditions. EOS, Trans Amer Geophys Union 77:S268 (abstract)
Wasserman E, Stixrude L, Cohen RE (1996b) Thermal properties of iron at high pressures and temperatures. Phys Rev B 53:8296-8309
Wentzcovitch RM (1991) Invariant molecular dynamics approach to structural phase transitions. Phys Rev B 44:2358-2361
Wentzcovitch RM, Martins JL, Price GD (1993) *Ab initio* molecular dynamics with variable cell shape: application to $MgSiO_3$ perovskite. Phys Rev Let 70:3947-3950
de Wijs GA et al. (1998) The viscosity of liquid iron at the physical conditions of the earth's core. Nature 392:805-807
Wolf GH, Bukowinski MST (1987) Theoretical study of the structural properties and equations of state of $MgSiO_3$ and $CaSiO_3$ perovskites: implications for lower mantle composition. *In:* High Pressure Research in Mineral Physics. Manghnani MH, Syono Y (eds), Terrapub, Tokyo p 313-331
Wood WW, Parker RF (1957) Monte Carlo equation of state of molecules interacting with the Lennard-Jones potential. I. Supercritical isotherm at about twice the critical temperature. J Chem Phys 27:720-733
Yoo CS, Holmes NC, Ross M, Webb DJ, Pike C (1993) Shock temperatures and melting of iron at earth core conditions. Phys Rev Let 70:3931-3934